Processing and Application of Ceramics 16 [4] (2022) 358–366
BY-NC-ND
https://doi.org/10.2298/PAC2204358S

Microstructure and mechanical properties of B_4C-TiB_2 composites reactive sintered from B_4C + TiO_2 precursors

Pavol Švec[1,*], Ľubomír Čaplovič[2]

[1]*Slovak University of Technology in Bratislava, Faculty of Mechanical Engineering, Institute of Technologies and Materials, Bratislava, Slovakia*
[2]*Slovak University of Technology in Bratislava, Faculty of Materials Science and Technology in Trnava, Institute of Materials Science, Trnava, Slovakia*

Received 21 June 2022; Received in revised form 8 September 2022; Accepted 21 October 2022

Abstract

Ceramic composites consisting of a boron carbide (B_4C) matrix and titanium diboride (TiB_2) secondary phase were obtained by reactive sintering from boron carbide powder with 40 and 50 wt.% of titanium dioxide (TiO_2) additive. The same sintering temperature of 1850 °C and pressure of 35 MPa, but different sintering times from 15 to 60 min, were applied during reactive hot pressing of the composites in vacuum. The effects of TiO_2 content and sintering time on phase compositions, microstructures and mechanical properties of the composites were studied. The TiO_2 additive enhanced densification of the B_4C-TiB_2 ceramic composites. Both Vickers hardness and the fracture toughness of the composites increased with prolongation of sintering time. The highest hardness of 29.8 GPa was achieved for the composite with 29.6 vol.% of TiB_2 obtained by sintering of the precursor with 40 wt.% of TiO_2 additive for 60 min. The fracture toughness reached a maximum value of 7.5 MPa·m$^{1/2}$ for the composite containing 40.2 vol.% of TiB_2, which was fabricated by reactive sintering of the precursor with 50 wt.% of TiO_2 additive for 60 min.

Keywords: *boron carbide, titanium diboride, ceramic composite, hardness, fracture toughness*

I. Introduction

Boron carbide (B_4C) is an important structural ceramic material with enhanced properties and promising industrial applications. B_4C ceramics is characterised by high melting point (2450 °C) and hardness (28–37 GPa) as it is the third hardest material after diamond and cubic boron nitride. It has low density (2.52 g/cm^3) and high Young's modulus (360–460 GPa) [1–5]. It has good impact and wear resistance, excellent resistance to chemical agents as well as high capacity for neutron absorption [4,6,7]. Based on these properties, B_4C ceramics is a perspective material for several applications. It is a promising candidate for wear resistance applications with abrasive or erosive wear such as cutting tools, blasting nozzles and water jet nozzles or for construction of light weight armour such as bullet-proof vests [8–11]. However, the application of B_4C has been limited by its low fracture toughness (1.2–3.7 MPa·m$^{1/2}$) and the poor sintering ability demanding relatively high sintering temperatures (above 2000 °C) [5,9,12,13].

Over the last few years, appropriate sintering additives were added to B4C initial powder to improve the sintering ability and mechanical properties of B_4C based ceramic materials. Numerous sintering aids have been identified that allow densification of B_4C ceramics at lower sintering temperature and production of B_4C based composites with secondary phases enhancing their fracture toughness. Primary sintering aids identified for B_4C include some metals (Ti, Zr, Nb, Al, Ni), oxides (TiO_2, ZrO_2, HfO_2, Al_2O_3, Y_2O_3), carbides (TiC, ZrC, NbC, TaC), nitrides (AlN, Si_3N_4) and diborides (TiB_2, ZrB_2, TaB_2, HfB_2). They are typically added in relatively high quantities, resulting in ceramic composites [13–18].

Composite materials consisting of B_4C matrix reinforced with titanium diboride (TiB_2) secondary phase have been considered as one of the most promising B_4C based ceramic composite materials, because of modifi-

*Corresponding author: tel: +421 2 57296 339
e-mail: *pavol.svec@stuba.sk*

cation of their properties by TiB_2 phase. TiB_2 is characterised by some superior properties including high melting point (3225 °C), high hardness (25–35 GPa), high Young's modulus (~450 GPa) and low density (4.52 g/cm^3). Its fracture toughness (3–5 MPa·m$^{1/2}$) is higher compared to B_4C [18,19]. Moreover, the presence of TiB_2 significantly reduces the electrical resistivity of B_4C based composites, enabling their electrical discharge machining [7]. The B_4C-TiB_2 ceramic composite materials can be prepared by non-reactive or reactive *in situ* sintering. The mixture of B_4C and TiB_2 initial powders is used in non-reactive sintering of B_4C-TiB_2 ceramic composites. However, the B_2O_3 and TiO_2 impurities on the surface of B_4C and TiB_2 starting powder strongly influence the densification behaviour and microstructure development of B_4C-TiB_2 ceramic composites [20–22]. The advantage of this sintering method is simple control of the final phase composition of the fabricated composite materials [7,23,24].

The initial mixtures of elemental powders (Ti, B, and C) or several powder mixtures (B_4C with TiC, B_4C with TiO_2 and B_4C with TiO_2 and C) enable the reactive sintering of B_4C-TiB_2 ceramic composites [7,25–31]. The advantage of reactive sintering is that the densification occurs at lower temperatures, which in comparison to non-reactive sintering leads to the formation of fine and well distributed *in situ* created TiB_2 secondary particles [1,7,26].

The reactive *in situ* sintering of B_4C powder with the TiO_2 sintering additive can be described by following reaction which is thermodynamically probable in temperature interval from 1300 to 1900 K [32,33]:

$$mB_4C + nTiO_2 \rightarrow oB_4C_{1-x} + pTiB_2 + qCO\uparrow \quad (\text{or } CO_2\uparrow) \qquad (1)$$

During the given reaction, sub-stoichiometric boron carbide B_4C_{1-x} and titanium diboride TiB_2 phases are created as a consequence of the reduction of TiO_2 sintering additive by carbon originating from the B_4C phase. In later stages of sintering process, the sub-stoichiometric boron carbide B_4C_{1-x} can reverse to the stoichiometric composition resulting in creation of the B_4C-TiB_2 composite materials. This is achieved by inward diffusion of carbon from external sources and by loss of excess boron through evaporation. The portion of *in situ* created TiB_2 phase is affected by sintering parameters, such as the concentration of TiO_2 additive, sintering temperature, and sintering time. The maximal amount of TiO_2 additive that can be added to B_4C without creation of free boron is 32 wt.% with CO being formed or 52 wt.% with CO_2 being formed in Eq. 1 [32,33].

The sintering method is a major factor that affects the densities, microstructures and mechanical properties of sintered B_4C-TiB_2 ceramic composites. Although pressureless sintering of B_4C-TiB_2 ceramics has been also studied, these composites could not reach the sufficient densification, which is a basic precondition for preparation of ceramic materials with unique mechanical properties [4,10,34]. Nearly full density in B_4C-TiB_2 ceramic composites can be achieved mainly by hot pressing, pulsed electric current sintering and spark plasma sintering [1,9,10,17,28,35]. Many authors have studied the effect of sintering parameters on the mechanical properties of B_4C-TiB_2 composites. Their results show that reactive *in situ* sintering is beneficial for densification of B_4C-TiB_2 ceramics. The reaction kinetics is influenced mainly by sintering additives, sintering temperature, applied pressure, and sintering time. Both the relative density of B_4C-TiB_2 ceramic composite and the portion of TiB_2 secondary phase generally increase with these parameters. However, higher sintering temperature or longer sintering time lead to coarsening of the microstructure [2,6]. Favourable mechanical properties were reported in fully dense B_4C-TiB_2 ceramic composites in several works and their values differ mainly depending on the portion of TiB_2 secondary phase. The portion of TiB_2 secondary phase enhances the fracture toughness of B_4C-TiB_2 composite, because of higher fracture toughness and toughening effect of TiB_2 phase utilising the toughening mechanisms, such as crack deflection, crack bridging and crack branching. However, higher portion of TiB_2 secondary phase could decrease the hardness, because of lower hardness of this phase compared to B_4C matrix [1,7,26,27].

Several authors prepared B_4C-TiB_2 composites by reactive hot pressing sintering of the same initial powder mixture consisting of B_4C, TiO_2 and graphite powders with different portion of TiB_2 phase in B_4C-TiB_2 composites and variable mechanical properties depending on the sintering parameters [7,26,27,29–31]. Khajehzadeh *et al.* [36] elaborated the thermodynamic of reaction occurring during sintering of this system and discussed the process of phase transformation in the B_4C-TiO_2-O system. Wang *et al.* [27] used reactive sintering at 2050 °C and 35 MPa for 1 h in vacuum of $1 \cdot 10^{-3}$ Pa. The B_4C-TiB_2 composites with 10 and 30 vol.% of TiB_2 reached the Vickers hardness of 29.5 and 28.0 GPa, respectively. The B_4C-TiB_2 composites with 40 vol.% of TiB_2 had fracture toughness of 8.2 MPa·m$^{1/2}$. Yamada *et al.* reactive sintered at 2000 °C and 50 MPa for 1 h and in 0.1 MPa Ar atmosphere. The B_4C-20%TiB_2 composite reached a strength of 866 MPa and fracture toughness of 3.2 MPa·m$^{1/2}$ [29]. Huang *et al.* [31] sintered B_4C-20%TiB_2 composite at 2000 °C and 25 MPa for 6 min. The resulting samples had a relative density, fracture toughness, and flexural strength of 99.9 %TD, 3.2 MPa·m$^{1/2}$, and 650 MPa, respectively. Skorokhod *et al.* [30] applied sintering temperature of 2000 °C at 20 MPa for 1 h in Ar atmosphere. The B_4C-TiB_2 composite with 15 vol.% of TiB_2 reached a strength of 621 MPa and fracture toughness of 6.1 MPa·m$^{1/2}$. Yue *et al.* [26] prepared the B_4C-43%TiB_2 composites by hot pressing of B_4C, TiO_2, and phenolic resin at 1950 °Cand 30 MPa, for 1 h in vacuum. The composites

had relative density, hardness, flexural strength and fracture toughness of 98.2 %TD, 25.9 GPa, 458 MPa and 8.7 MPa·m$^{1/2}$, respectively [26]. In the work of Failla *et al.* [7], the B_4C-TiB_2 composites were hot pressed from B_4C, TiB_2 and WC at 1860 °C, 30 MPa for 10–20 min in vacuum of 0.1 mbar. The B_4C-TiB_2 composite with 25 vol.% of TiB_2 showed the hardness of 32.2 GPa, whereas the B_4C-TiB_2 composite with 75 vol.% TiB_2 had the fracture toughness of 5.01 MPa·m$^{1/2}$ [7]. Zhao *et al.* [1] sintered B rich B_xC-TiB_2 composites from TiC-B mixtures at 2000 °C and 35 MPa for 1 h in a dynamic vacuum. The maximal Vickers hardness was 30.4 GPa and the fracture toughness was 5.78 MPa·m$^{1/2}$ [1]. As these values are quite different, more information about the microstructures and mechanical properties of B_4C-TiB_2 composites are needed.

Based on the results from our previous works [37,38], the B_4C-TiB_2 composites prepared from B_4C + TiO_2 precursors with 40 to 50 wt.% TiO_2 sintered at 1850 °C under pressure of 35 MPa in vacuum of about 10 Pa have the relative densities above 99 %TD and favourable combination of mechanical properties. These composites were sintered for 60 min and therefore it is reasonable to study properties of B_4C-TiB_2 composites sintered for shorter times. Consequently, the presented work focused on the effects of sintering time on the microstructure, density, hardness and fracture toughness of B_4C-TiB_2 ceramic composite materials and the relationship between sintering parameters and properties of the B_4C-TiB_2 composites.

II. Experimental

B4C and TiO_2 powders with the purity of 99% and particle size from 2 to 3 µm were used to fabricate B_4C-TiB_2 ceramic composites. Powder mixtures consisting of B_4C with 40 and 50 wt.% TiO_2 (used as sintering additive) were homogenised in horizontal mill in Teflon container of 450 ml volume with B_4C mill balls and isobutyl alcohol. The initial powder mixtures were preliminary consolidated using die pressing at a pressure of about 130 MPa in a simple tool with a floating die of cylindrical shape with a diameter of 8 mm. The final consolidation was realized using hot pressing in a graphite die with a floating matrix of cylindrical shape with a diameter of 8 mm at sintering temperature of 1850 °C, pressure of 35 MPa and different sintering time from 15 to 60 min in a vacuum. The abbreviation BT40-*x* and BT50-*x* were used for the composites prepared from the precursor B_4C powder with 40 and 50 wt.% TiO_2, respectively, where *x* corresponds to sintering time, i.e. 15, 30, 45 and 60 min.

The phase analysis was performed using XRD on Philips PW 1710 diffractometer with source of characteristic X-ray of CoKα operated at 40 kV and 40 mA in the 2θ range from 20° to 100° with a step of 0.026° and scan step time of 47 s. The microstructures were observed using JEOL JSM IT300 scanning electron microscope. Volume portions of the formed phases were estimated using image analysis with the Multiphase module of AxioVision software. The densities of the hot pressed samples were measured using the Archimedes' method. The relative bulk density was calculated based on the results of phase identification from the XRD analysis and measured volume portion of phases from the image analysis. The theoretical densities were calculated according to the rule of mixture using the density values of pure phases: 2.52 g/cm^3 for B_4C and 4.52 g/cm^3 for TiB_2. The hardness and fracture toughness were measured using a Vickers indenter with load of 5 kgf (49.03 N) and indentation time of 10 s. The fracture toughness K_{IC} of the B_4C-TiB_2 ceramic composites was calculated using the formula proposed by Shetty [39]:

$$K_{IC} = 0.0889\left(\frac{H \cdot F}{4a}\right)^{1.2} \tag{2}$$

where H is the hardness, F is the applied force, and a is the average radial crack length measured on the impression.

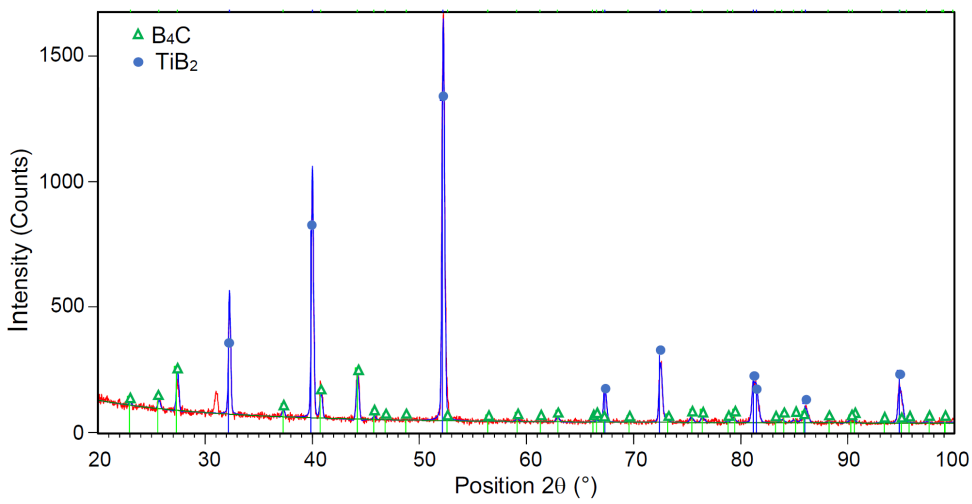

Figure 1. XRD pattern of the BT40-60 composite reactively hot pressed at 1850 °C for 60 min

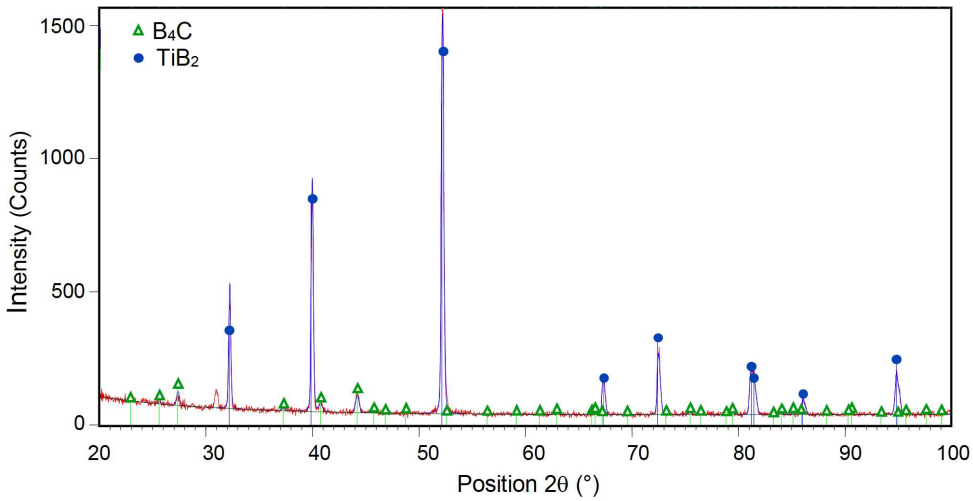

Figure 2. XRD pattern of the BT50-60 composite reactively hot pressed at 1850 °C for 60 min

III. Results and discussion

3.1. Microstructure of B_4C-TiB_2 composites

XRD patterns of the composites prepared by reactive sintering of the B_4C + TiO_2 precursors with 40 and 50 wt.% TiO_2 for 60 min are presented in Figs. 1 and 2, respectively. Only two phases were detected: matrix B_4C and secondary TiB_2 phase. The signal intensity ratio of the TiB_2/B_4C phases for the BT40-60 composite (Fig. 1) is lower compared to that of the BT50-60 composite (Fig. 2). This is the consequence of a higher portion of the secondary TiB_2 phase created in the BT50-60 compared to the BT40-60 composite. The formation of the same phases was observed also for the samples sintered for different times. The sub-stoichiometry of B_4C_{1-x} was not measured during the XRD analysis of the prepared composite samples.

Microstructures of the BT40-*x* composites sintered for different times are presented in Fig. 3. Three different areas can be identified in the microstructure of the BT40-15 composite (Fig. 3a). The B_4C matrix is represented by the grey areas. The secondary TiB_2 phase with the portion of 24.3 vol.% is represented by the light areas. The dark areas with the portion of 9.2 vol.% represent the residual porosity. The portions of TiB_2 phase and porosity were measured using the image analysis. The same phases, but with different portions, were observed in the microstructures of all investigated samples. It can be seen from Fig. 3 that porosity of the composites decreases with the prolongation of the sintering time. Significant decrease of porosity below 1 vol.% with simultaneous increase of the portion of the secondary TiB_2 phase to 28.2 vol.% was observed after sintering for 45 min (Fig. 3b). Fully dense microstructure (without visible porosity) with 29.6 vol.% of TiB_2 phase was obtained in the composite BT40-60, sintered for 60 min.

The identification of microstructures of the B_4C-TiB_2 composites was supported by the elemental mapping analysis. Mapping analysis of the B_4C-TiB_2 composite BT40-60 reactively sintered for 60 min is presented in Fig. 4. Higher magnification was chosen to distinguish the distribution of elements in the composite phases. The distributions of B in Fig. 4a and Ti in Fig. 4c supported by XRD analysis in Fig. 1 confirm the identification of the matrix B_4C (grey areas) and secondary TiB_2 (light areas) phase in Fig. 4b.

Similar effect of sintering time on microstructure observed for the BT40-*x* composites was visible for the BT50-*x* samples (Fig. 5). Thus, microstructure of the

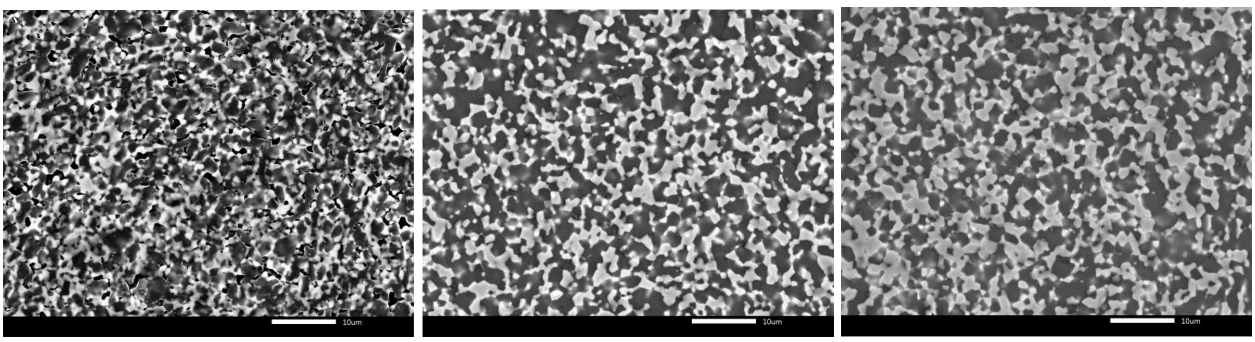

(a) (b) (c)

Figure 3. Microstructure of B_4C-TiB_2 composites: a) BT40-15 with 24.3 vol.% TiB_2 hot pressed for 15 min, b) BT40-45 with 28.2 vol.% TiB_2 hot pressed for 45 min and c) BT40-60 with 29.6 vol.% TiB_2 hot pressed for 60 min

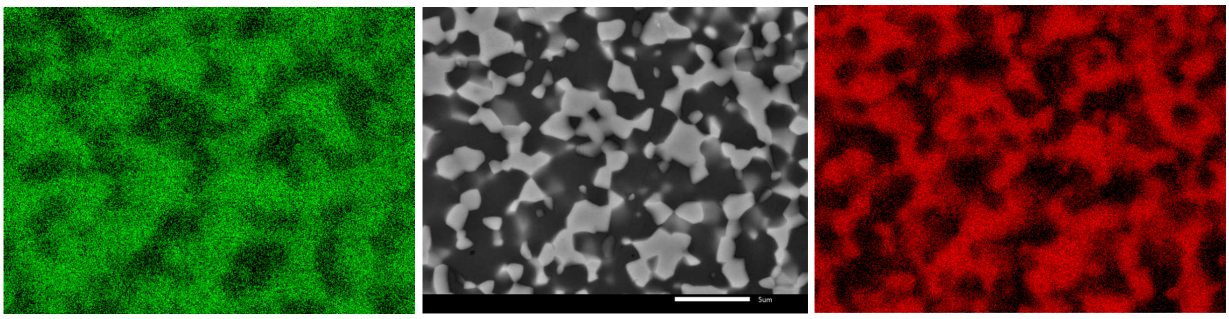

(a) (b) (c)

Figure 4. Elemental mapping analysis of B_4C-TiB_2 composite BT40-60 reactively hot pressed for 60 min: a) distribution of B ($K_{\alpha 1\text{-}2}$), b) corresponding SEM image and c) distribution of Ti ($K_{\alpha 1}$)

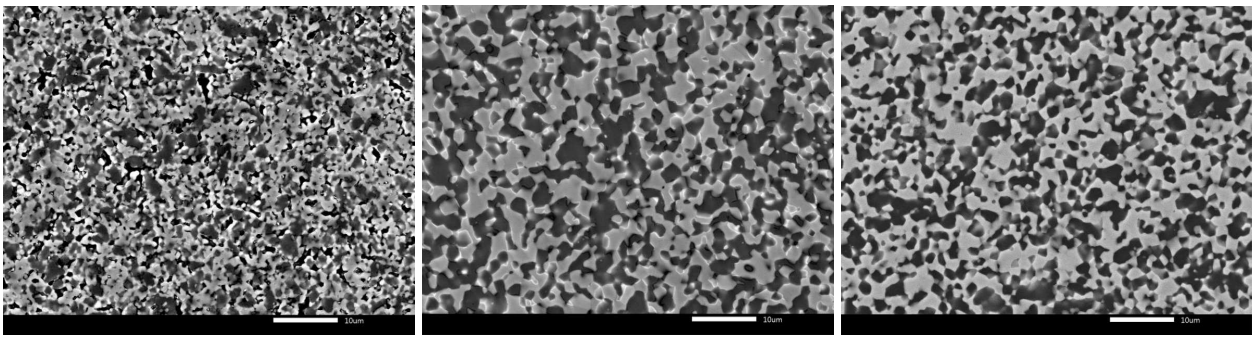

(a) (b) (c)

Figure 5. Microstructure of B_4C-TiB_2 composites: a) BT50-15 with 37.2 vol.% TiB_2 hot pressed for 15 min, b) BT50-45 with 39.3 vol.% TiB_2 hot pressed for 45 min and c) BT50-60 with 40.2 vol.% TiB_2 hot pressed for 60 min

BT50-*x* composites consists of the B_4C matrix, TiB_2 secondary phase and porosity. The portions of TiB_2 phase (light areas) increase with sintering time. Uniform decrease of porosity with the prolongation of the sintering time was observed in both types of composites prepared by sintering of two different initial powder mixtures. However, higher portions of the secondary TiB_2 phase were formed in the BT50-*x* composites than in the BT40-*x* samples sintered for identical sintering time. Both ceramic composites reactively sintered for 60 min (Figs. 3c and 5c) are without visible porosity, but an apparently higher portion of TiB_2 secondary phase is created in the B_4C-TiB_2 composite prepared from the B_4C + 50 wt.% TiO_2 precursor.

The effect of both the initial powder mixture composition and sintering time on TiB_2 secondary phase portion formed in the B_4C-TiB_2 composites during reactive hot pressing at the temperature of 1850 °C and pressure of 35 MPa is presented in Fig. 6. Almost linear progress of secondary phase portion created in B_4C-TiB_2 composites with sintering time can be seen for both types of composites (BT40-*x* and BT50-*x*). Higher portion of the secondary TiB_2 phase in the hot pressed BT50-*x* composites is related to the larger extent of the *in situ* reaction during sintering. The maximal portion of TiB_2 secondary phase (40.2 vol.%) was measured by the image analysis of the sample sintered for the longest time (60 min).

Figure 7 reveals the effects of sintering time on density of the ceramic composites hot pressed at 1850 °C

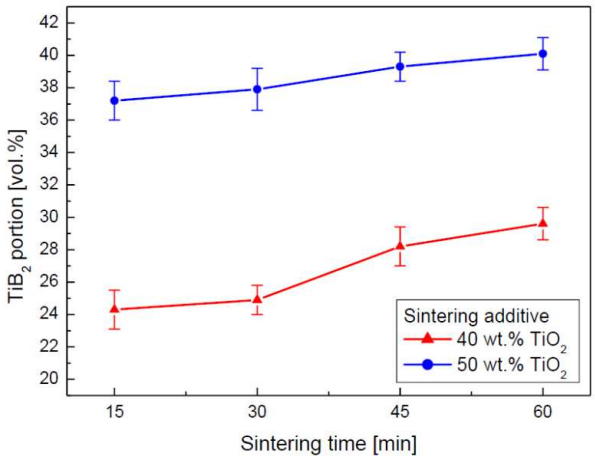

Figure 6. The effect of sintering time on portion of secondary TiB_2 phase in hot pressed B_4C-TiB_2 composites

and pressure of 35 MPa. Figure 7 confirms the increase of density with the prolongation of sintering time and similar behaviour for both samples. Relative densities of the hot pressed BT40-*x* composites are slightly lower than that of the BT50-*x* samples, but the measured values overlap partially. The BT40-*x* samples reached the average densities from 90.8 to 99.3 %TD when prolonging sintering time from 15 to 60 min. Higher standard deviation in the density values was measured at sintering time of 15 min, because of higher porosity of those composites. The average densities of the sintered BT50-

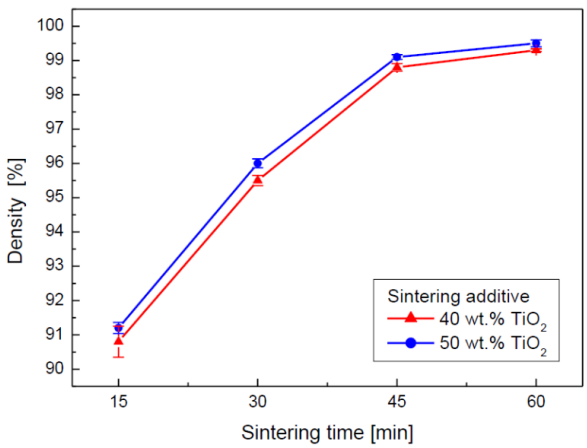

Figure 7. The effect of sintering time on density of B_4C-TiB_2 composites

x samples increased from 91.2 to 99.5 %TD with the prolongation of sintering time from 15 to 60 min. As nearly full density was measured for both samples sintered for 60 min, longer sintering time was not applied.

3.2. Mechanical properties of B_4C-TiB_2 composites

The effect of sintering time on the hardness of B_4C-TiB_2 composites is shown in Fig. 8. The average hardness value of the BT40-*x* samples increased from 15.4 to 29.8 GPa when prolonging sintering time from 15 to 60 min. Significant increase in the hardness of the composites was observed in sintering time interval from 30 to 45 min. The highest measured hardness value was 29.8 GPa and it was achieved for the B_4C-TiB_2 composite with 29.6 vol.% of TiB_2 phase. The average hardness of the BT50-*x* composites increased from 22.6 to 28.5 GPa with the prolongation of sintering time from 15 to 60 min. Significant increase in the hardness of these composites was observed when prolonging sintering time from 15 to 30 min.

The obtained hardness values of the B_4C-TiB_2 composites (Fig. 8) was influenced by two factors: the densification progress and portion of TiB_2. The densification showed the crucial effect on hardness increase at sintering times up to 30 min, whereas the portion of the formed TiB_2 phase was dominant from sintering times longer than 45 min. The densification was enhanced by the concentration of sintering additive (TiO_2) in the precursor powders. This was the reason for higher hardness of the BT50-*x* composites sintered at shorter sintering times, up to 30 min, compared to the BT40-*x* samples. At longer sintering times, above 45 min, both composites achieved required densification with density values about 99 %TD. From this sintering stage higher portion of TiB_2 *in situ* created phase in the BT50-60 composite resulted in its lower hardness compared to the sample fabricated from the precursors with 40 wt.% TiO_2.

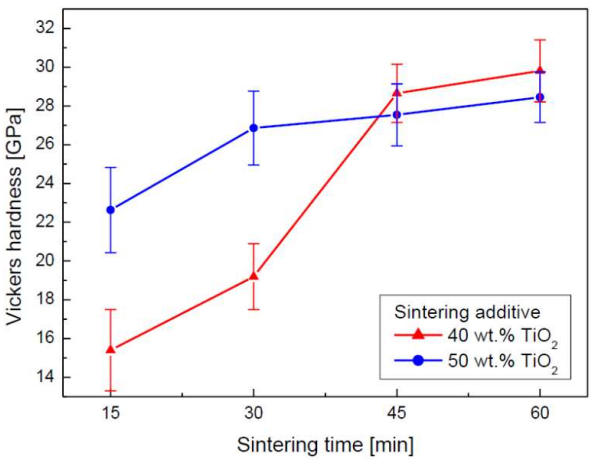

Figure 8. The effect of sintering temperature on the hardness of hot pressed B_4C-TiB_2 composites

The hardness values of 29.8 GPa and 28.5 GPa were measured for fully densified (above 99.3 %TD) B_4C-TiB_2 ceramic composites with 29.6 and 40.2 vol.% of TiB_2 secondary phase, respectively. These values show hardness decrease with the increase of TiB_2 portion in B_4C-TiB_2 composites sintered for identical time of 60 min. This can be compared with the results reported in previous works [7,26,27], where the hardness values of 32.2 GPa [7], 29.5 GPa [27], 28.0 GPa [27] and 25.9 GPa [26] were measured for B_4C-TiB_2 ceramic composites with 10, 25, 30 and 43 vol.% of TiB_2 phase, respectively.

Figure 9 shows Vickers indentation morphology of the BT50-60 composite reactively hot pressed for 60 min. The B_4C matrix is represented by the grey areas and the secondary TiB_2 phase with the portion of 40.2 vol.% is represented by the light areas. The radial cracks initiating from the corners of impression are visible and measured length (*a*) of one crack is marked in Fig. 9.

The effect of sintering time on the fracture toughness of the hot pressed B_4C-TiB_2 composites is shown in Fig. 10. The average fracture toughness of the BT40-

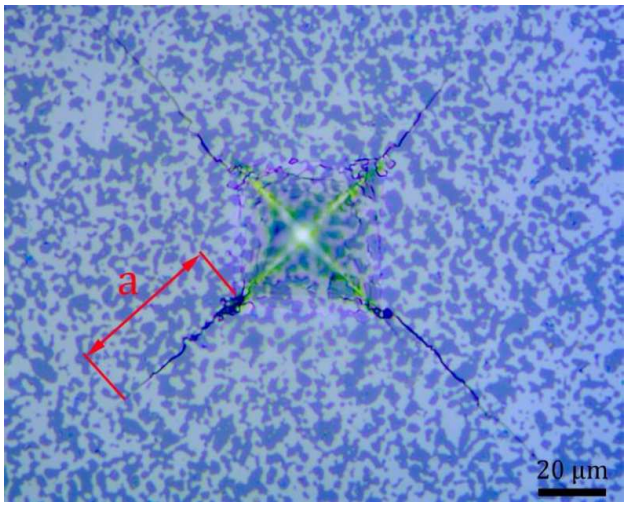

Figure 9. Vickers indentation morphology of B_4C-TiB_2 composite reactively hot pressed for 60 min (*a* is measured length of one radial crack)

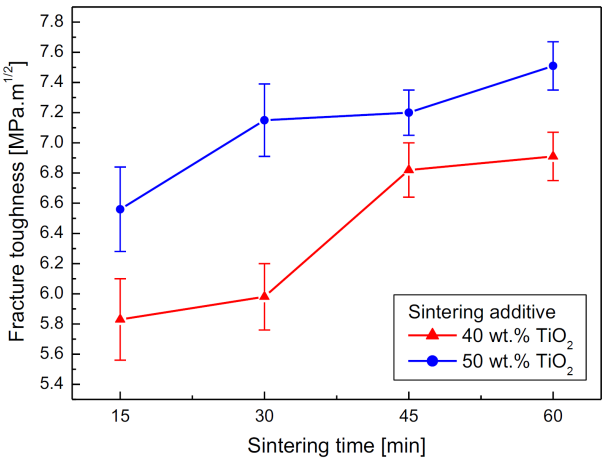

Figure 10. The effect of sintering temperature on the fracture toughness of hot pressed B_4C-TiB_2 composites

x composites increased from 5.8 to 6.9 MPa·m$^{1/2}$ when prolonging sintering time from 15 to 60 min. The average fracture toughness of the BT50-*x* composites increased from 6.6 to 7.5 MPa·m$^{1/2}$ when prolonging sintering time from 15 to 60 min. Higher values of fracture toughness were achieved for the BT50-*x* samples compared to the BT40-*x* samples. This can be explained by the formation of a higher portion of the toughening TiB_2 secondary phase in the BT50-*x* samples compared to the BT40-*x* samples. The earlier densification of the precursors having higher concentration of TiO_2 (50 wt.%) was reflected in a similar way as it was described when the progress of hardness was discussed in Fig. 8. Significant increase of the fracture toughness of the sintered BT50-*x* composites was observed when sintering time was increased from 15 to 30 min. However, the increase of the fracture toughness of the sintered BT40-*x* composites was postponed to sintering times interval from 30 to 45 min. The highest fracture toughness of 7.5 MPa·m$^{1/2}$ was measured for the B_4C-TiB_2 composite with the highest portion of TiB_2 (40.2 vol.%) toughening phase.

The fracture toughness values could be compared with the literature data: 3.2 [29,31], 8.2 [27] and 8.7 MPa·m$^{1/2}$ [26] achieved for the B_4C-TiB_2 ceramic composites with 20, 40 and 43 vol.% of secondary TiB_2 phase, respectively. These values confirmed the positive effect of TiB_2 phase on toughening effect in B_4C-TiB_2 ceramics and in this work we achieved the fracture toughness values of 6.9 and 7.5 MPa·m$^{1/2}$ for the B_4C-TiB_2 fully dense ceramic composites (99.3 and 99.5 %TD) with 29.6 and 40.2 vol.% of TiB_2 phase, respectively.

IV. Conclusions

B_4C-TiB_2 ceramic composites were hot pressed using *in situ* reaction of two initial powder mixtures consisting of B_4C with 40 and 50 wt.% of TiO_2 at 1850 °C, under pressure of 35 MPa and in a vacuum for different sintering time (15, 30, 40 and 60 min). The effects of sintering time and amount of TiO_2 in precursor powders on the microstructure, density, hardness and fracture toughness of the ceramic composites were studied.

All composite samples consisted of two phases, B_4C matrix and TiB_2 secondary phase. The portion of TiB_2 phase created in the B_4C-TiB_2 composites increased with the prolongation of sintering time. The positive effect of sintering time on the density was observed for both types of the samples achieving values above 99 %TD for the longest sintering time of 60 min.

The densification was crucial for the hardness increase at sintering times up to 30 min. It was enhanced in the samples fabricated from the precursor with higher concentration of TiO_2 (50 wt.% TiO_2). However, the higher portion of softer TiB_2 phase caused lower hardness of the composite with higher concentration of TiO_2 (50 wt.% TiO_2). The highest hardness value of 29.8 GPa was achieved for the B_4C-TiB_2 composite with 29.6 vol.% of TiB_2 phase obtained from the precursor with 40 wt.% TiO_2 and sintered for the longest time of 60 min.

Higher values of fracture toughness were achieved for the samples fabricated with higher portion of TiO_2 sintering additives. This can be explained by the formation of a higher portion of TiB_2 toughening secondary phase in these composites. The highest fracture toughness of 7.5 MPa·m1$^{/2}$ was measured for the B_4C-TiB_2 composite with the highest portion of 40.2 vol.% TiB_2 phase.

Acknowledgements: This work was supported by UVP STU Bratislava the ITMS 26240220084 project and the 313021BXZ1 project.

References

1. J. Zhao, C. Tang, Q. Li, Z. Liu, S. Ran, "B_4C-TiB_2 composites fabricated by hot pressing TiC-B mixtures: The effect of B excess", *Ceram. Int.*, **48** [9] (2022) 11981–11987.
2. T. Tian, L. Hu, A. Wang, C. Liu, W. Guo, P. Xu, Q. He, W. Wang, H. Wang, Z. Fu, "Fabrication and characterization of hot-pressed B-rich boron carbide", *Ceram. Int.*, **48** [12] (2022) 16505–16515.
3. E.A. Weaver, B.T. Stegman, R.W. Trice, J.P. Youngblood, "Mechanical properties of room-temperature injection molded, pressurelessly sintered boron carbide", *Ceram. Int.*, **48** [8] (2022) 11588–11596.
4. K. Ye, T. Prikhna, C. Hu, Z. Wang, "Morphology characteristics and mechanical properties of hot-pressed micron/sub-micron boron carbide ceramics," *Mater. Today Commun.*, **29** (2021) 102751.
5. R. Belon, G. Antou, N. Pradeilles, A. Maitre, D. Gosset, "Mechanical behaviour at high temperature of spark plasma sintered boron carbide ceramics", *Ceram. Int.*, **43** [8] (2017) 6631–6635.
6. B.M. Moshtaghioun, M.A. Laguna-Bercero, D. Gomez-García, J.I. Pena, "Does grain size have an influence on intrinsic mechanical properties and conduction mechanism of near fully-dense boron carbide ceramics", *J. Alloys Compd.*, **795** (2019) 408–415.
7. S. Failla, C. Melandri, L. Zoli, G. Zucca, D. Sciti, "Hard

and easy sinterable B_4C-TiB_2-based composites doped with WC", *J. Eur. Ceram. Soc.*, **38** [9] (2018) 3089–3095.
8. Y. Gao, T. Tang, C. Yi, W. Zhang, D. Li, W. Xie, W. Huang, N. Ye, "Study of static and dynamic behavior of TiB_2-B_4C composite", *Mater. Des.*, **92** (2016) 814–822.
9. X. Zhang, Z. Zhang, B. Nie, H. Chen, Y. Wang, L. Zheng, Y. Bai, W. Wang, "Microstructure and mechanical properties of fine-grained boron carbide ceramics fabricated by high-pressure hot pressing combined with high-energy ball milling", *Ceram. Int.*, **44** [9] (2018) 10766–10772.
10. X. Zhang, Z. Zhang, R. Wen, G. Wang, X. Zhang, J. Mu, H. Che, W. Wang, "Comparisons of the densification, microstructure and mechanical properties of boron carbide sintered by hot pressing and spark plasma sintering", *Ceram. Int.*, **44** [2] (2018) 2615–2619.
11. J. Hu, F. Zhang, W. Wang, Z. Fu, J. Zhang, "Effect of impurities introduced by ball milling on hot pressed boron carbide", *J. Eur. Ceram. Soc.*, **39** [9] (2019) 2874–2881.
12. M. Khajehzadeh, H.R. Baharvandi, N. Ehsani, S. Verma, M. Bahaaddini, N.K. Batra, "Experimental investigation and validation on the effect of nickel addition on properties of the pressureless sintered boron carbide composites using machine learning models", *Ceram. Int.*, **48** [9] (2022) 13205–13215.
13. Y. Zhu, F. Wang, Y. Wang, H. Cheng, D. Luo, Y. Zhao, "Mechanical properties and microstructure evolution of pressureless-sintered B_4C-SiC ceramic composite with CeO_2 additive", *Ceram. Int.*, **45** [12] (2019) 15108–15115.
14. K. Ye, Z. Wang, "Twins enhanced mechanical properties of boron carbide", *Ceram. Int.*, **48** [10] (2022) 14499–14506.
15. N. Barbakadze, L. Chkhartishvili, A. Mikeladze, O. Tsagareishvili, K. Sarajishvili, T. Korkia, M. Darchiashvili, L. Rurua, N. Jalabadze, R. Chedia, "Method of obtaining multicomponent fine-grained powders for boron carbide matrix ceramics production", *Mater. Today Proc.*, **51** [5] (2022) 1863–1871.
16. G. Liu, S. Chen, Y. Zhao, Y. Fu, Y. Wang, "The effect of transition metal carbides MeC (Me = Ti, Zr, Nb, Ta, and W) on mechanical properties of B_4C ceramics fabricated via pressureless sintering", *Ceram. Int.*, **46** [17] (2020) 27283–27291.
17. X. Zhang, H. Gao, Z. Zhang, R. Wen, G. Wang, J. Mu, H. Che, X. Zhang, "Effects of pressure on densification behaviour, microstructures and mechanical properties of boron carbide ceramics fabricated by hot pressing", *Ceram. Int.*, **43** [8] (2017) 6345–6352.
18. Z. Fu, R. Koc, "Microstructure and mechanical properties of hot pressed submicron TiB_2 powders", *Ceram. Int.*, **44** [8] (2018) 9995–9999.
19. D. Wang, S. Ran, L. Shen, H. Sun, Q. Huang, "Fast synthesis of B_4C-TiB_2 composite powders by pulsed electric current heating TiC-B mixture", *J. Eur. Ceram. Soc.*, **35** [3] (2015) 1107–1112.
20. S.G. Huang, K. Vanmeensel, O.J.A. Malek, O. Van der Biest, J. Vleugels "Microstructure and mechanical properties of pulsed electric current sintered B_4C-TiB_2 composites", *Mater. Sci. Eng. A*, **528** [3] (2011) 1302–1309.
21. W.S. Rubink, W. Ageh, H. Lide, N.A. Ley, M.L. Young, D.T. Casem, E.J. Faierson, W. Scharf "Spark plasma sintering of B_4C and B_4C-TiB_2 composites: Deformation and failure mechanisms under quasistatic and dynamic loading", *J. Eur. Ceram. Soc.*, **41** [6] (2021) 3321–3332.
22. Z. Liu, X. Deng, J. Li, Y. Sun, S. Ran, "Effects of B_4C particle size on the microstructures and mechanical properties of hot-pressed B_4C-TiB_2 composites", *Ceram. Int.*, **44** [17] (2018) 21415–21420.
23. I. Bogomol, H. Borodianska, T. Zhao, T. Nishimura, Y. Sakka, P. Loboda, O. Vasylkiv, "A dense and tough (B_4C-TiB_2)-B_4C composite within a composite produced by spark plasma sintering", *Scripta Mater.*, **71** (2014) 17–20.
24. J. Wu, B. Niu, F. Zhang, L. Lei, J. Zhang, L. Ren, W. Wang, Z. Fu, "Effect of titanium diboride on the homogeneity of boron carbide ceramic by flash spark plasma sintering", *Ceram. Int.*, **44** [13] (2018) 15323–15330.
25. Z. Liu, D. Wang, J. Li, Q. Huang, S. Ran, "Densification of high strength B_4C-TiB_2 composites fabricated by pulsed electric current sintering of TiC-B mixture", *Scripta Mater.*, **135** (2017) 15–18.
26. X.Y. Yue, S.M. Zhao, L. Yu, H.Q. Ru, "Microstructures and mechanical properties of B_4C-TiB_2 composite prepared by hot pressure sintering", *Key Eng. Mater.*, **434-435** (2010) 50–53.
27. Y. Wang, H. Peng, F. Ye, Y. Zhou, "Effect of TiB_2 content on microstructure and mechanical properties of in-situ fabricated TiB_2/B_4C composites", *Trans. Nonferrous Met. Soc. China*, **21** (2011) 369–373.
28. S.G. Huang, K. Vanmeensel, O. Van der Biest, J. Vleugels, "In situ synthesis and densification of submicrometer-grained B_4C-TiB_2 composites by pulsed electric current sintering", *J. Eur. Ceram. Soc.*, **31** [4] (2011) 637–644.
29. S. Yamada, K. Hirao, Y. Yamauchi, S. Kanzaki, "High strength B_4C-TiB_2 composites fabricated by reaction hot-pressing", *J. Eur. Ceram. Soc.*, **23** [7] (2003) 1123–1130.
30. V. Skorokhod, V.D. Krstic, "High strength-high toughness B_4C-TiB_2 composites", *J. Mater. Sci. Lett.*, **19** (2000) 237–239.
31. S.G. Huang, K. Vanmeensel, J. Vleugels, "Powder synthesis and densification of ultrafine B_4C-ZrB_2 composite by pulsed electrical current sintering", *J. Eur. Ceram. Soc.*, **34** [8] (2014) 1923–1933.
32. L. Levin, N. Frage, M.P. Dariel, "A novel approach for the preparation of B_4C-based cermets", *Int. J. Refr. Met. Hard Mater.*, **18** [1] (2000) 131–135.
33. L. Levin, N. Frage, M.P. Dariel, "The effect of Ti and TiO_2 additions on the pressureless sintering of B_4C", *Metall. Trans.*, **30A** [1] (1999) 3201–3210.
34. B. Matović, V. Urbanovich, V. Girman, M. Lisnichuk, D Nikolić, J. Erčić, J.I. Cvijović–Alagić, "Densification of boron carbide under high pressure", *Mater. Lett.*, **314** (2022) 131877.
35. B. Niu, F. Zhang, J. Zhang, W. Ji, W. Wang, Z. Fu, "Ultra-fast densification of boron carbide by flash spark plasma sintering", *Scripta Mater.*, **116** (2016) 127–130.
36. M. Khajehzadeh, N. Ehsani, H.R. Baharvandi, A. Abdollahi, M. Bahaaddini, A. Tamadon, "Thermodynamical evaluation, microstructural characterization and mechanical properties of B_4C-TiB_2 nanocomposite produced by in-situ reaction of nano-TiO_2", *Ceram. Int.*, **46** [17] (2020) 26970–26984.
37. P. Švec, Z. Gábrišová, A. Brusilová, "Microstructure and mechanical properties of B_4C-TiB_2 ceramic composites hot pressed with in-situ reaction", *J. Ceram. Process. Res.*, **20** [1] (2019) 113–120.
38. P. Švec, Z. Gábrišová, A. Brusilová, "Reactive sintering of B_4C-TiB_2 composites from B_4C and TiO_2 precursors",

Process. Appl. Ceram., **14** [4] (2020) 329–335.
39. D.K. Shetty, I.G. Wright, P.N. Mincer, A.H. Clauer, "Indentation fracture of WC-Co cermets", *J. Mater. Sci.*, 20 (1985) 1873–1882.